Cell Reports, Volume *40*

Supplemental information

Runx2 regulates chromatin accessibility to direct the osteoblast program at neonatal stages

Hironori Hojo, Taku Saito, Xinjun He, Qiuyu Guo, Shoko Onodera, Toshifumi Azuma, Michinori Koebis, Kazuki Nakao, Atsu Aiba, Masahide Seki, Yutaka Suzuki, Hiroyuki Okada, Sakae Tanaka, Ung-il Chung, Andrew P. McMahon, and Shinsuke Ohba

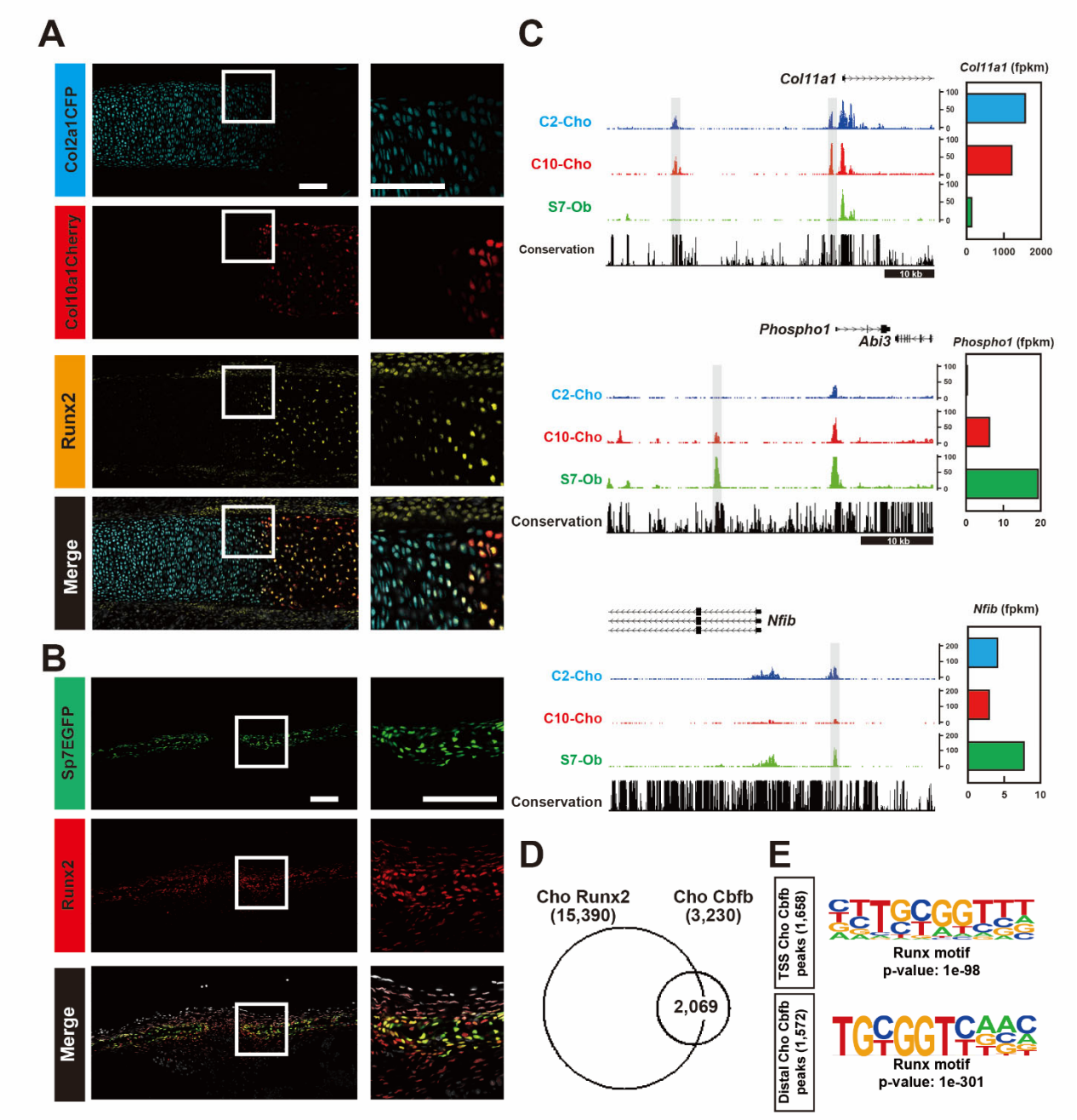

Figure S1 (related to Figures 1 and 2). Reporter activities and ATAC-seq profiles of Col2a1-ECFP, Col10a1-mCherry, and Sp7-EGFP, Runx2 expression, and interactions of Runx2 and Cbfβ in genome.

(**A,B**) Native expression of reporter fluorescence and immunohistochemistry for Runx2 of the ribs and calvariae at P1. Col2a1-ECFP and Col10a1-mCherry double transgenic mice were used for rib staining (A). Sp7-EGFP was used for calvarial staining (B). DAPI (white) indicates the nucleus in the merged images. Enlargement of the boxed regions is shown. Representative images obtained from biological duplicates are shown. Scale bar: 100 μm.

(**C**) CisGenome browser screenshots showing chromatin accessibility (left) and the corresponding gene expression in skeletal cell types (right). Peaks highlighted in gray indicate chromatin accessible regions shared between C2-Cho and C10-Cho in the flanking regions of *Col11a1* (upper panel); an accessible region shared between C10-Cho and S7-Ob in the flanking regions of *Phospho1* (middle panel); and an accessible region shared between C2-Cho and S7-Ob in the

flanking regions of *Nfib* (lower panel). Representative data obtained from biological triplicates (left) and normalized values from biological triplicates (right) are shown.

(**D**) Venn diagram showing the overlap between Runx2 ChIP-seq peaks and Cbfβ ChIP-seq peaks in P1 chondrocytes. Numbers of each ChIP-seq peaks and the overlapped peaks are shown.

(**E**) *De novo* motif analysis of Cbfβ ChIP-seq peaks. TSS peaks and distal peaks were defined as peaks < 500 bp from the nearest TSS, and > 500 bp from the nearest TSS, respectively. Peak numbers in each data sets and the p-value of motifs are shown.

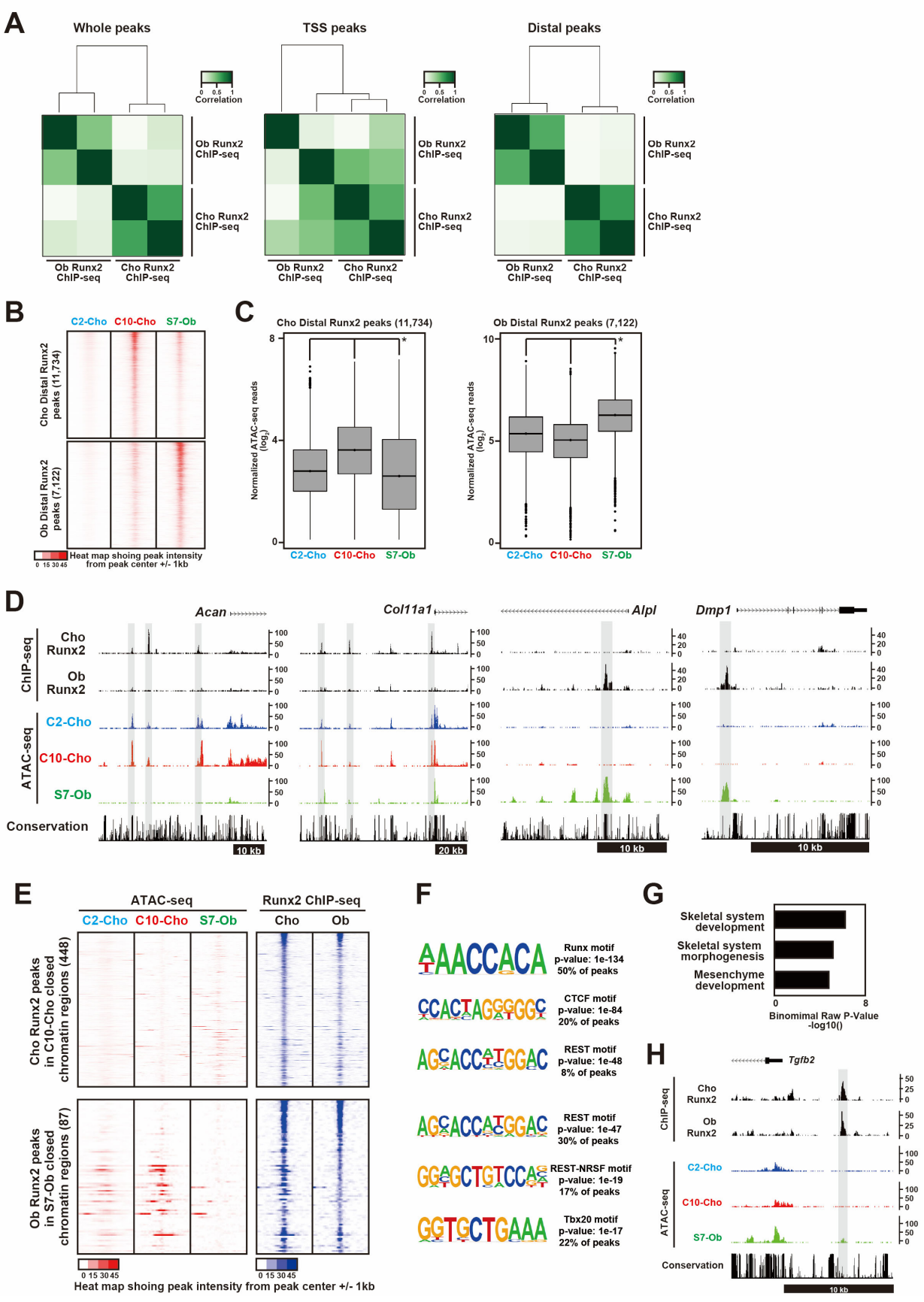
A
Whole peaks
TSS peaks
Distal peaks
Correlation
Ob Runx2 ChIP-seq
Cho Runx2 ChIP-seq
B
C2-Cho C10-Cho S7-Ob
Cho Distal Runx2 peaks (11,734)
Ob Distal Runx2 peaks (7,122)
Heat map shoing peak intensity from peak center +/- 1kb
C
Cho Distal Runx2 peaks (11,734)
Ob Distal Runx2 peaks (7,122)
Normalized ATAC-seq reads (log2)
D
Acan
Col11a1
Alpl
Dmp1
ChIP-seq
ATAC-seq
Cho Runx2
Ob Runx2
C2-Cho
C10-Cho
S7-Ob
Conservation
E
ATAC-seq
Runx2 ChIP-seq
Cho Runx2 peaks in C10-Cho closed chromatin regions (448)
Ob Runx2 peaks in S7-Ob closed chromatin regions (87)
Heat map shoing peak intensity from peak center +/- 1kb
F
Runx motif p-value: 1e-134 50% of peaks
CTCF motif p-value: 1e-84 20% of peaks
REST motif p-value: 1e-48 8% of peaks
REST motif p-value: 1e-47 30% of peaks
REST-NRSF motif p-value: 1e-19 17% of peaks
Tbx20 motif p-value: 1e-17 22% of peaks
G
Skeletal system development
Skeletal system morphogenesis
Mesenchyme development
Binomimal Raw P-Value -log10()
H
Tgfb2

Figure S2 (related to Figure 2 and 3). Comparison analysis of Runx2–DNA binding signatures between chondrocytes and osteoblasts and associations with chromatin signatures in skeletal cell types.

(**A**) Correlation analysis of Runx2–DNA associations in between chondrocytes and osteoblasts. Signal intensities in the whole Runx2 ChIP-seq peaks (left), those in the regions located within 500 bp from the nearest TSS regions (TSS peaks), and those in the distal regions far more than 500 bp from the nearest TSS regions (Distal regions) were used. Color indicator represents correlations among profiles in normalized read counts. Profiles of biological duplicates were ised.

(**B, C**) Heatmaps (B) and box plots (C) showing signal intensities of the indicated ATAC-seq in the distal Runx2 peak regions in chondrocytes and osteoblasts. Color indicator represents intensity of the normalized reads in the ATAC-seq profiles. In Figure S2C, y-axis value is $\log_2$ (normalized reads +1). *$p < 0.01$ vs. normalized reads in biological triplicates with the one factor-associated site (Tukey-HSD analysis).

(**D**) CisGenome browser screenshots showing the cell type-distinct Runx2 binding regions and the chromatin accessibility.

(**E**) Heatmaps showing signal intensities of chromatin accessibility and Runx2-DNA binding in the Runx2 peaks at the closed chromatin regions in chondrocytes and osteoblasts. 488 regions of chondrocyte Runx2 peaks at closed chromatin regions in Col10-positive chondrocytes (C10-Cho), and 87 regions of osteoblast Runx2 peaks at closed regions in Sp7-positive osteoblasts (S7-Ob) were extracted. The color indicator represents the intensity of the normalized reads in the ATAC-seq profiles (left) and Runx2 ChIP-seq profiles (right).

(**F**) *De novo* motif analysis of the selected regions is shown in (E). The top three enriched motifs are shown.

(**G**) GREAT GO annotations of the chondrocyte Runx2 peaks, having the Runx consensus motif at closed chromatin regions in C10-Cho cells. The top three enriched terms are shown.

(**H**) CisGenome browser screenshot showing a Runx2 peak at closed chromatin regions.

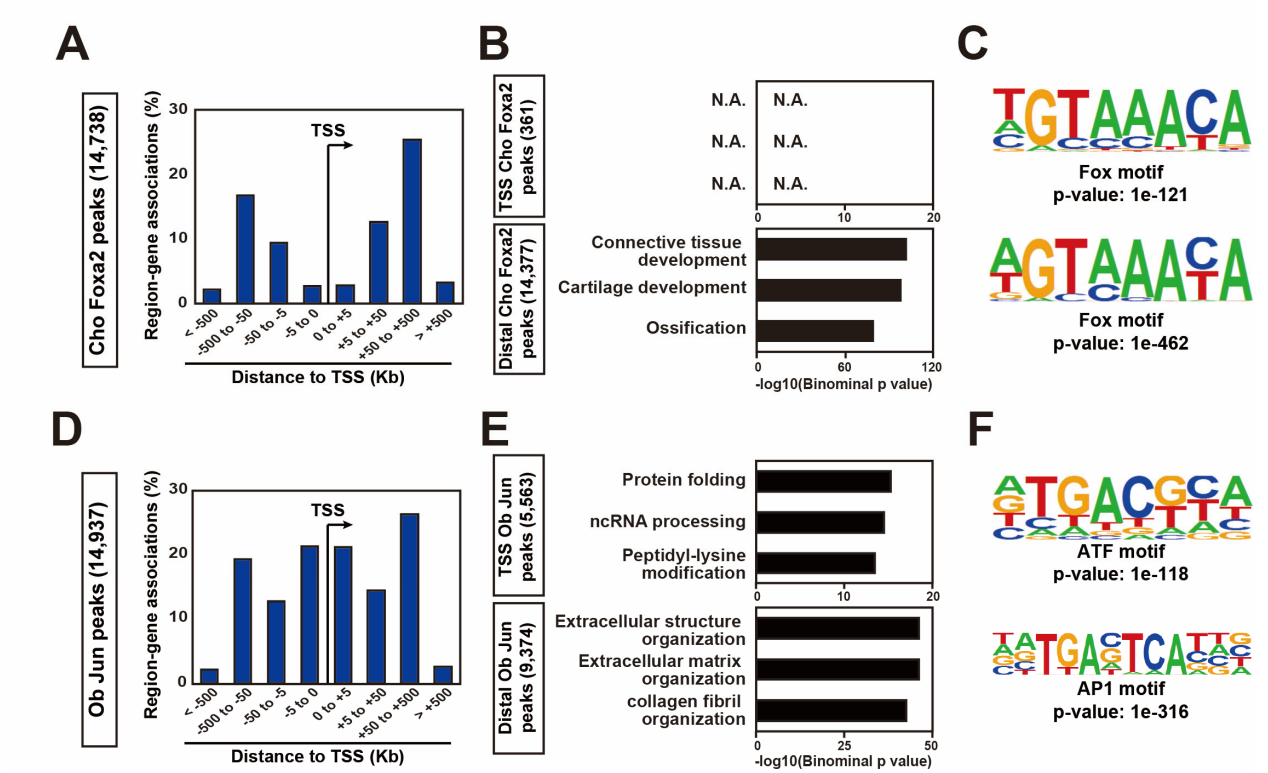

Figure S3 (related to Figure 3). ChIP-seq studies for chondrocyte Foxa2 and osteoblast Jun.

(**A**) Genome-wide distribution of Foxa2-associated regions relative to TSSs in chondrocytes (Cho). The total number of Foxa2-associated regions is indicated.

(**B**) GREAT GO annotations of Foxa2-associated regions showing the top three enriched terms. TSS regions and distal regions were separately analyzed.

(**C**) *De novo* motif analysis of top 1,000 Foxa2-associated regions in chondrocytes. The most enriched motif is shown.

(**D**) Genome-wide distribution of Jun-associated regions relative to transcriptional start sites (TSSs) in osteoblasts (Ob). The total number of Jun-associated regions is indicated.

(**E**) GREAT GO annotations of Jun-associated regions showing the top three enriched terms. TSS regions and distal regions were separately analyzed.

(**F**) *De novo* motif analysis of top 1,000 Jun-associated regions in osteoblasts. The most enriched motif is shown.

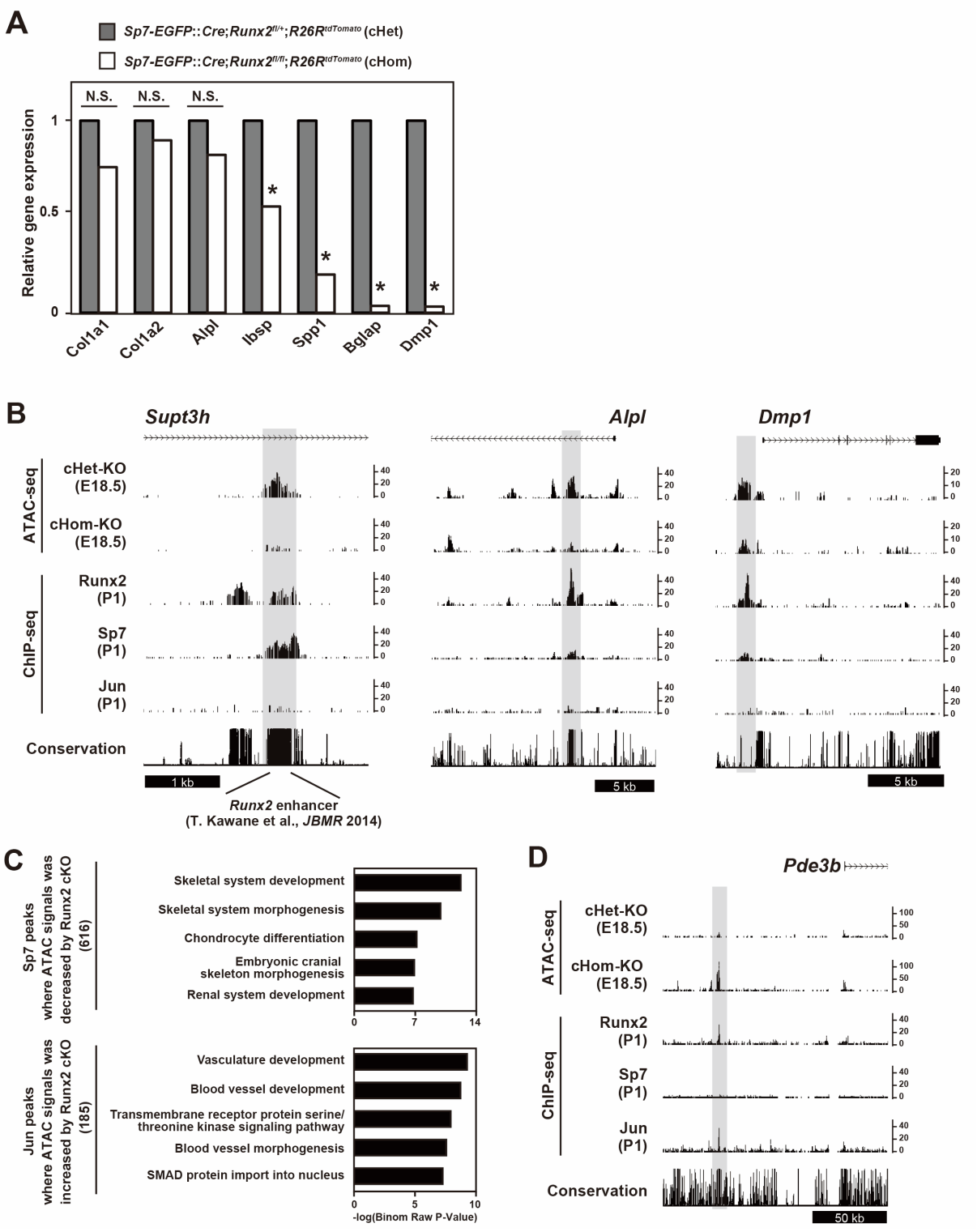

Figure S4 (related to Figure 4). Effects of *Runx2* ablation on gene expression and chromatin accessibility in osteoblasts.

(**A**) Gene expression analysis of *Runx2* cHet-KO and cHom-KO mice at E18.5 by RNA-seq analysis. cHet and cHom indicate tdTomato-positive cells sorted from *Sp7-EGFP*::*Cre*;*Runx2*$^{fl/+}$;*R26R*^{tdTomato} calvarias, and *Sp7-EGFP*::*Cre*;*Runx2*$^{fl/fl}$;*R26R*^{tdTomato} calvarias, respectively. Relative gene expression is shown. *$p < 0.05$; N.S.: not

significant. Normalized values from biological duplicates were used.

(**B**) CisGenome browser screenshots showing regions with the significantly decreased chromatin accessibility by Runx2 deficiency. ChIP-seq for Runx2-BioFL, Sp7-BioFL and Jun in P1 osteoblasts were followed.

(**C**) GREAT GO annotations of the osteoblasts Sp7 peaks (upper panel) and Jun peaks (lower panel) where ATAC signals was significantly decreased by Runx2 cKO. The top five enriched terms are shown.

(**D**) A CisGenome browser screenshot showing the significantly increased chromatin accessible regions by Runx2 deficiency. ChIP-seq signals for Runx2-BioFL, Sp7-BioFL and Jun in P1 osteoblasts are also shown.

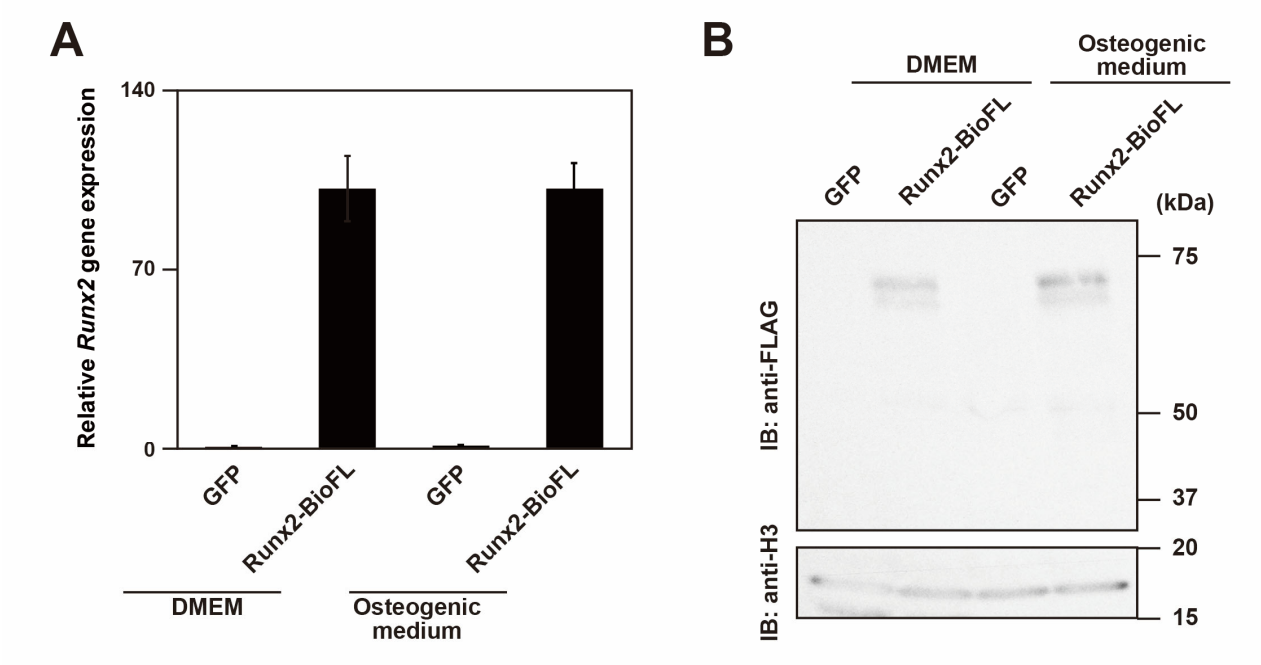

Figure S5 (related to Figure 5). mRNA and protein expression of Runx2-BioFL in NIH3T3 cells.

Runx2 mRNA expression was determined by RT-qPCR (A) and Runx2 protein expression was determined by western blot (B) in NIH3T3 fibroblast cells overexpressing GFP or Runx2-BioFL. Cells were cultured with either DMEM or an osteogenic medium for 3 days. In (A), data are presented as the means ± SD of triplicate experiments. Blotting for Histone H3 (H3) was used for the control.

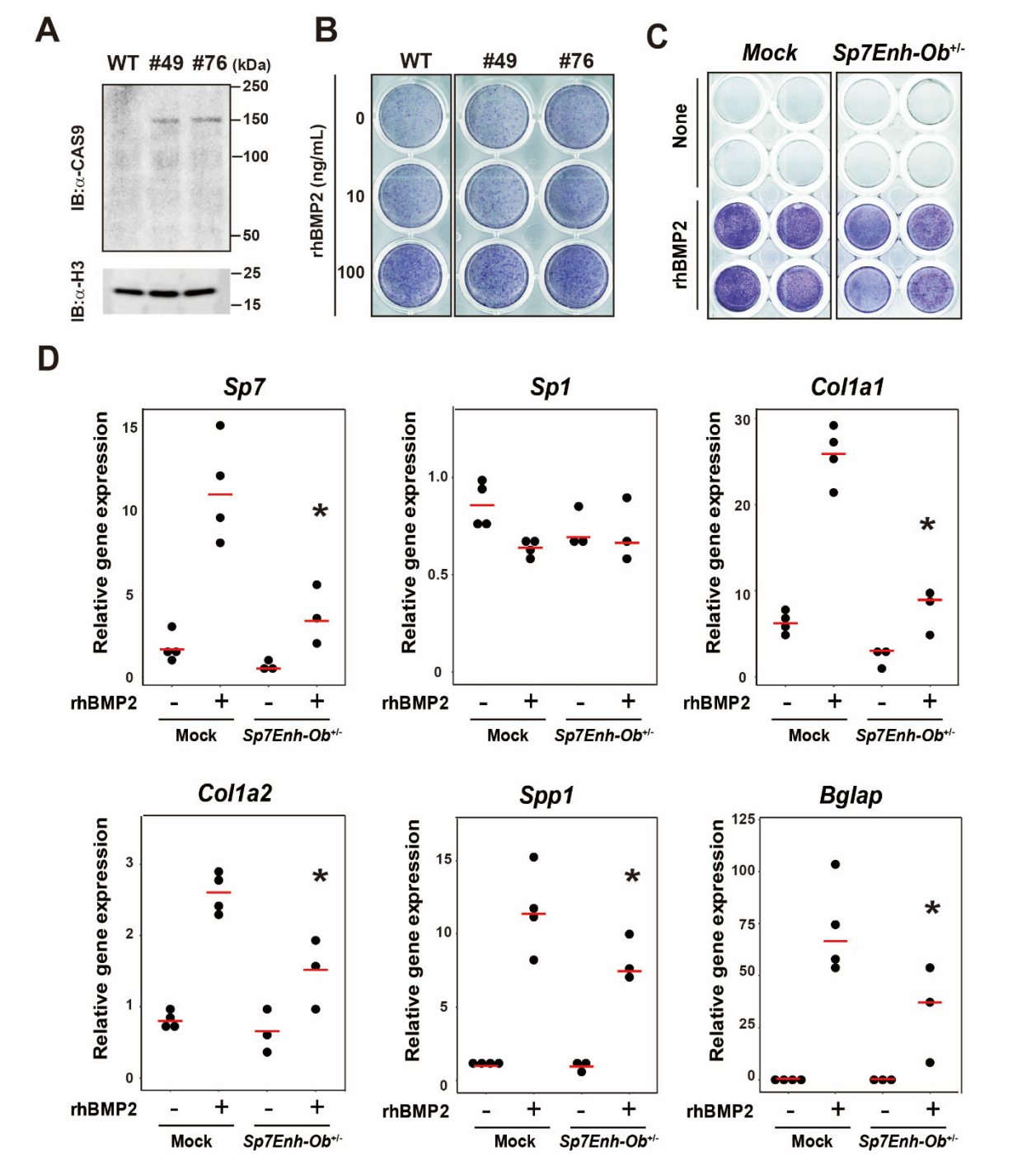

Figure S6 (related to Figures 6 and 7). Osteoblast differentiation in *Sp7Enh-Ob* deficient MC3T3-E1 cells.

(**A**) Western blot for the expression of CAS9 protein in Cas9-stable MC3T3-E1 clones. CAS9 protein was detected at approximately 150 kDa in clones #49 and #76.

(**B**) Alkaline phosphatase staining of Cas9-stable MC3T3E1 clones. Cells were cultured in the osteogenic medium with the indicated concentrations of rhBMP2 for 7 days. Staining intensity was increased in a rhBMP2-dependent manner regardless of the clones, suggesting that osteoblast differentiation is not attenuated by Cas9-stable expression. We used the clone #76 in experiments shown in Figure 6.

(**C**) Alkaline phosphatase staining of Sp7 enhancer-knockout (*Sp7Enh-Ob*$^{+/-}$) and the control MC3T3-E1 cells (Mock).

Enhancer-knockout cells were generated using the CRISPR-Cas9 system with dual guide RNA expressions targeting the Sp7 enhancer. Cells were cultured in the osteogenic medium with 50 ng/ml rhBMP2 for 10 days. Staining intensity was decreased in *Sp7Enh-Ob*$^{+/-}$ cells compared to the control.

(**D**) Expression of *Sp7*, *Sp1,* and osteoblast marker genes in *Sp7Enh-Ob*$^{+/-}$ MC3T3-E1 cells relative to the control (Mock). Cells were cultured in the osteogenic medium with or without 50 ng/ml rhBMP2 for 10 days. Each dot represents gene expression in each clone averaged by technical triplicates; red lines represent the average gene expression. **P* < 0.05 vs. mock cells with rhBMP2 treatment.

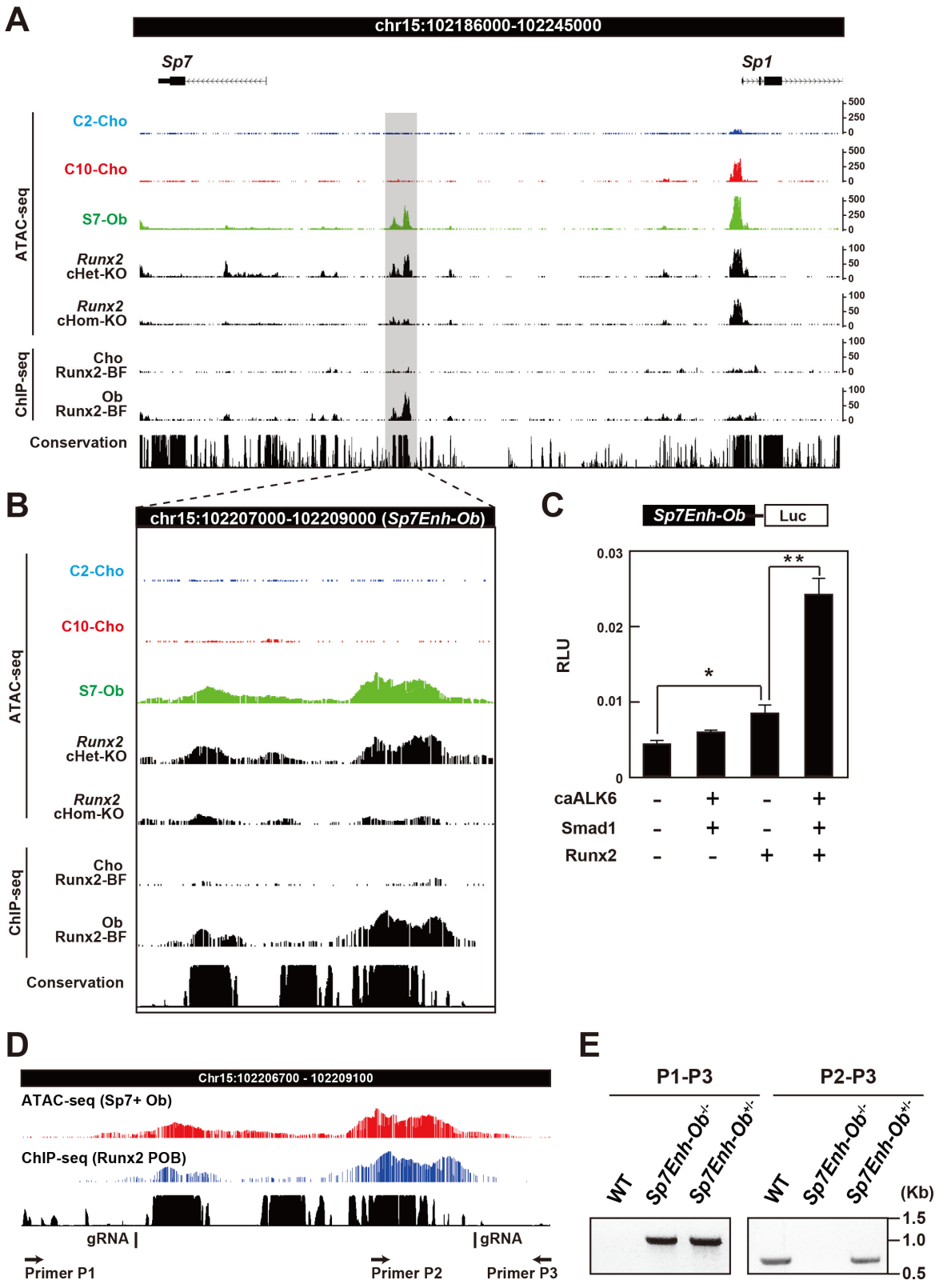

Figure S7 (related to Figure 6 and 7). Chromatin accessibilities and Runx2–DNA binding profiles in the *Sp7Enh* and generation of *Sp7Enh-Ob* knockout mouse.

(**A,B**) CisGenome browser screenshot showing chromatin accessibility and Runx2–DNA binding profiles in the flanking

regions of *Sp7* and *Sp1*. The identified *Sp7* enhancer region is highlighted in (A) and enlarged in (B).

(**C**) Luciferase assay for the Sp7 enhancer activity. Different combinations of the indicated plasmid DNA were transfected into 293T cells. Data, i.e., relative light unit (RLU), are presented as the means ± SD of triplicate experiments. caALK6; constitutive active form of ALK6. *$p < 0.05$; **$p < 0.01$

(**D**) CisGenome browser screenshot of the flanking region of the *Sp7* enhancer and the experimental schematic diagram for the design of gRNAs and genotyping primers.

(**E**) PCR genotyping analysis of *Sp7Enh-Ob* knockout mouse. P1 and P3 primers yielded amplification products of approximately 1 kb in length, P2 and P3 primers, 600 bp.